Spherulitic Growth and Cellulation in Dilute Blends of Monodisperse Long *n*-Alkanes

I. L. Hosier, D. C. Bassett,* and A. S. Vaughan

J. J. Thomson Physical Laboratory, University of Reading, Reading RG6 6AF, U.K.

Received May 31, 2000

ABSTRACT: Dilute blends of two guest monodisperse *n*-alkanes one, *n*-$C_{122}H_{246}$, shorter and one, *n*-$C_{246}H_{494}$, longer than the pure host, *n*-$C_{162}H_{326}$, have been investigated regarding the kinetics and morphology of both spherulitic growth and cellulation to clarify the related phenomena in polymers. All samples were crystallized isothermally between 118 and 124 °C. For the pure material this gave the optical textures expected of chain-extended crystallization, i.e., objects which may display circular envelopes but differ from classic spherulites in that they have domains of uniform crystallographic orientation. With increasing crystallization temperature these objects become larger and coarser to a limit when they are no more than aggregates of single crystals. Addition of 5% or 10% of a second component to *n*-$C_{162}H_{326}$ lowers growth rates and drastically alters morphologies. When the guest is longer than the host, there is cocrystallization producing permanent cilia and finer-textured, radially symmetric spherulites. When it is shorter, it segregates with a decelerating growth rate akin to observations of cellulation in branched polyethylenes. The resulting solids have disrupted crystallographic ordering and textures with randomly oriented lamellae. In all cases, adjacent dominant lamellae splay apart by angles which increase linearly with supercooling. The rate of increase is less for blends than for the pure host and the magnitudes increase with guest concentration being greatest when there is both permanent and transient ciliation. Positive intercepts at zero supercooling may indicate a supplementary contribution from surface roughness of the embryonic lamella. The combined observations provide strong confirmation of the importance of ciliation in promoting spherulitic growth of long molecules, independent of segregation and cellulation.

Introduction

It is remarkable that, although universally recognized as the characteristic mode of polymeric crystallization from the melt,[1] spherulitic growth and its molecular causes have remained problematic since the first observations[2] more than 50 years ago until relatively recently. For a long time, the lack of detailed morphological knowledge allowed alternative suggestions to survive without close scrutiny. When detailed morphology could be studied, it suggested, initially in concentrated solutions[3] and later from the melt, that the cause was ciliation, namely the uncrystallized portions of molecules partly attached to growing crystals, which repelled nearest neighbor lamellae. The evidence suggesting this in melt-grown systems was, first, the regular splaying of adjacent dominant lamellae[4,5] and then the divergence of successive layers of a spiral terrace around a giant screw dislocation.[6] These observations show unambiguously that the divergence is due to a mesoscopically short-range repulsion, operative over no longer than the molecular length. Confirmation that this force is indeed a consequence of ciliation became possible with the availability of the monodisperse *n*-alkanes.[7,8]

The tendency of these molecules to crystallize with their methyl end groups in lamellar basal surfaces[9] leads to quantized lamellar thicknesses and the opportunity of a clear test of the role of ciliation. To the approximation that stems add to a layer as integral units, transient ciliation will be absent for extended-chain growth but present when only one stem is attached in once-folded growth. The corresponding morphologies precisely matched the expected correlation of ciliation and spherulites with the demonstration in *n*-$C_{294}H_{590}$ that the interlamellar packing is dramatically different in the two cases.[10,11] In the once-folded form there is divergence and branching of dominant lamellae giving spherulites analogous to those in polymers, but for extended growth the texture is one of wide expanses of parallel lamellae. This is striking confirmation of the responsibility of ciliation for lamellar divergence and thence spherulitic growth.

Subsequent work on the monodisperse long *n*-alkanes has examined the fine details of extended-chain growth,[12,13] specifically the development of lamellar divergence and pseudo-spherulites at higher supercoolings, showing that this is most likely due to the addition of chains progressively to a lamella rather than as the oversimplification of whole stems. The suggestion is that, as the length of the secondary nucleus decreases at higher supercooling, so transient ciliation, due to the excess of molecular length over that of the nucleus, will develop and increase. Supporting evidence comes from measurements showing that lamellar divergence increases linearly with supercooling, i.e., proportional to the length of an extended cilium.[13] Nevertheless, the existence and role of transient ciliation has to be inferred from indirect evidence and the phenomenon is not under direct experimental control.

In this paper, we investigate systems in which it is possible to introduce and control the number of permanent cilia in the crystallizing system, in addition to the inherent transient ones which will disappear if and when a molecule is fully incorporated in a lamella. These can be generated using a dilute cocrystallizing blend in which the minority guest molecule is longer than the host. As expected, such systems crystallize

* Author for correspondence.

10.1021/ma000946t CCC: $19.00
Published on Web 10/28/2000

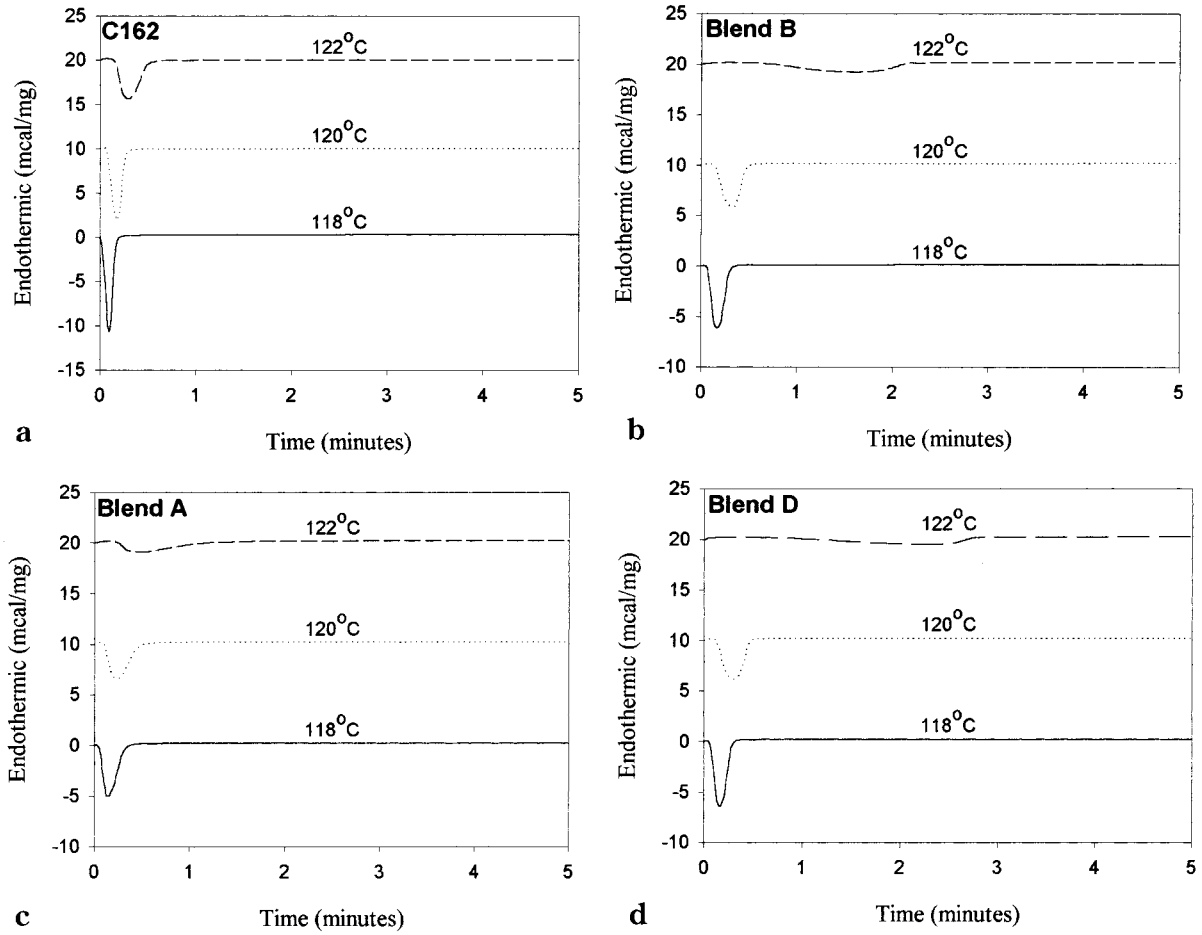

Figure 1. Isothermal DSC crystallization exotherms at the indicated temperatures from (a) C162, (b) blend A, (c) blend B, and (d) blend D.

Table 1. Compositions of the Blends Used in This Investigation

	major component			minor component		
blend	material	mass (%)	molar (%)	material	mass (%)	molar (%)
A	$C_{162}H_{326}$	94.5	93.3.	$C_{122}H_{246}$	5.5	6.7
B	$C_{162}H_{326}$	94.6	96.6	$C_{246}H_{494}$	5.4	3.4
C	$C_{162}H_{326}$	90.2	87.3	$C_{122}H_{246}$	9.8	12.7
D	$C_{162}H_{326}$	89.8	93.1	$C_{246}H_{494}$	10.2	6.9

more slowly than the pure host and give profuse finely textured spherulites. Complementary blends in which the guest molecule is shorter than the host show, when crystallized above the melting point of the guest alkane, both slowed kinetics and segregation leading to coarse pseudo-spherulitic habits. These observations provide further detailed confirmation of the causal role of ciliation in generating spherulites of long-chain molecules and of the independence of spherulitic growth from cellulation.

Experimental Section

Nomenclature. Four blends based on *n*-$C_{162}H_{326}$ were employed in this study, denoted blends A−D. Blends A and C contained, respectively, approximately 5% and 10 wt % of *n*-$C_{122}H_{246}$, while blends B and D contained, respectively, approximately 5% and 10% of *n*-$C_{246}H_{494}$; the exact compositions are listed in Table 1. For convenience, these three pure *n*-alkanes, studied in detail previously,[13] will henceforth be referred to as C122, C162, and C246.

Blending Procedure. A 50 mg sample of each blend was prepared as follows: the required amounts of each paraffin were weighed out into new vials on a Stanton DSC microbalance and then dissolved in 10 mL of BDH "Aristar" brand xylene (99.9% purity) heated to its boiling point under constant stirring. Meanwhile about 10 mL of methanol (BDH "Aristar" brand) was cooled over dry ice and, after some 10 min, the hot solution was poured into the methanol, producing immediate precipitation of the paraffin blend. This was removed from the solvent by filtration, then dried under vacuum until no further mass loss was recorded; the recovered powder was stored in a sealed vial until ready for use. The homogeneity of the blends was checked by melting ∼1 mg portions and comparing their endotherms to pure C162 and to each other.

Thermal Analysis. Melting and crystallization of the blends were monitored with a Perkin-Elmer DSC-2C differential scanning calorimeter (DSC), calibrated for isothermal and scanning runs against tin, indium, lead and stearic acid. For crystallization runs, samples of ∼1−2 mg in a DSC pan, were melted at 134 °C for 1 min, then cooled at 40 K min^{-1} to the required isothermal crystallization temperature. Data of heat flow against time enabled the time for crystallization and the associated enthalpy change to be calculated. Immediately following crystallization, the sample pan was quenched on a cold surface. Melting endotherms of the product were recorded at a heating rate of 20 K min^{-1}. To avoid problems of degradation, no more than two runs were carried out for each fresh specimen and always under a nitrogen atmosphere.

Optical Microscopy and Growth Kinetics. The same sample was used to obtain both the optical micrographs and the kinetic measurements. Around 5 mg of the required paraffin or blend was placed between a clean microscope slide and coverslip and the whole inserted into a Mettler FP80 hotstage. The material was melted at 134 °C for 1 min, and was then cooled at 40 K min^{-1} to the required crystallization temperature, so as closely to duplicate the thermal conditions

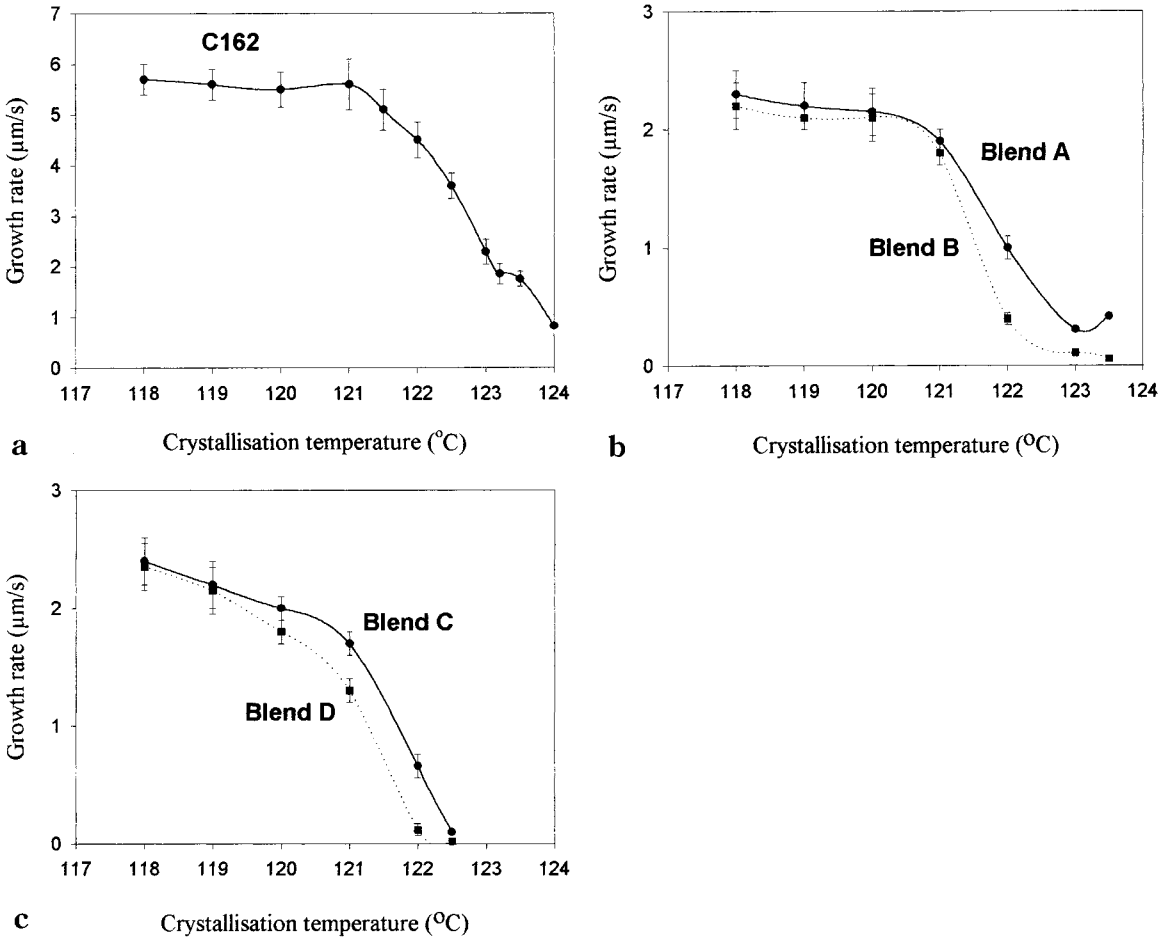

Figure 2. Growth rates as a function of crystallization temperature for (a) C162, (b) blends A and B, and (c) blends C and D.

of the DSC runs. In situ imaging of crystals was obtained by placing the hot-stage between crossed polars on a Vickers microscope and using a small CCD video camera for recording as crystallization proceeded. Kinetic data were obtained directly by marking the tips of individual crystals on the monitor screen at successive times and taking the gradients of the fitted curves of dimension vs time. In many cases the growth rate was constant as crystallization advanced, yielding a single average growth rate at each crystallization temperature. However, in certain blends, the growth rate decreased with time; in such cases the single growth rate figure used refers to the average initial gradient of the dimension/time plots of individual objects. Optical micrographs were recorded in transmission between crossed polars immediately after full crystallization; their magnifications were calibrated against a standard graticule.

Transmission Electron Microscopy, TEM. The morphology of the paraffins was examined using TEM, via carbon replicas to circumvent beam damage. Because of limited availability of materials, the specimen was crystallized directly between the squares of a gold TEM grid (200 mesh) and a direct replica was taken. To this end both sample and grid were placed on a clean microscope slide and the specimen was premelted on a Kofler hot bench so it filled the grid and excluded any air bubbles. A prewarmed coverslip was placed on top and the whole assembly was crystallized in the hot-stage as detailed above. Following crystallization, the coverslip was removed and the whole assembly was etched for 10 min in a pool of permanganic reagent, which was changed halfway through the procedure. The reagent was prepared beforehand by dissolving 1% (w/v) $KMnO_4$ in an acid mix composed of 1 part water, 4 parts orthophosphoric acid, and 10 parts sulfuric acid. Reaction was quenched by soaking in a mixture of 1 part hydrogen peroxide in an acid mixture composed of 2 parts sulfuric acid to 7 parts water which had been cooled over dry ice for at least 10 min beforehand. The grid was then washed with methanol, gently lifted from the slide, and allowed to dry.

To prepare the replica, tungsten/tantalum metal was evaporated on the etched surface at ~35° to the horizontal, followed by vertical carbon coating. Finally the paraffin was removed from the grids by refluxing in boiling xylene, leaving the grids ready for examination.

X-ray Procedure. Small-angle X-ray scattering was used to measure the crystal thickness of the blends and to compare it to pure C162. The single diffraction ring obtained in each case corresponded to the length of the extended chain of C162, with molecules being inclined at 35° to the lamellar normal. It follows that the small amount of C122 or C246 introduced into the blends left the structure of the C162 crystals essentially unchanged.

Results: Crystallization and Growth Kinetics

Crystallization Behavior. Crystallization exotherms for pure C162, and three of the blends (A, B, and D) are shown as parts a−d of Figure 1, respectively. For clarity, only a few exotherms are shown, at three representative crystallization temperatures.

A comparison of pure C162 with any of the blends for any given temperature (Figure 1) shows that the crystallization times of the blends are around twice those of the pure material, increasing with concentration of the minor component. At 118 and 120 °C, the crystallization times and shapes of the exotherms for all the blends are very similar, even in changing from 5% to 10% C246 (cf. Figure 1, parts c and d).

At 122 °C, the distinction between different blends becomes more apparent. When the minority component

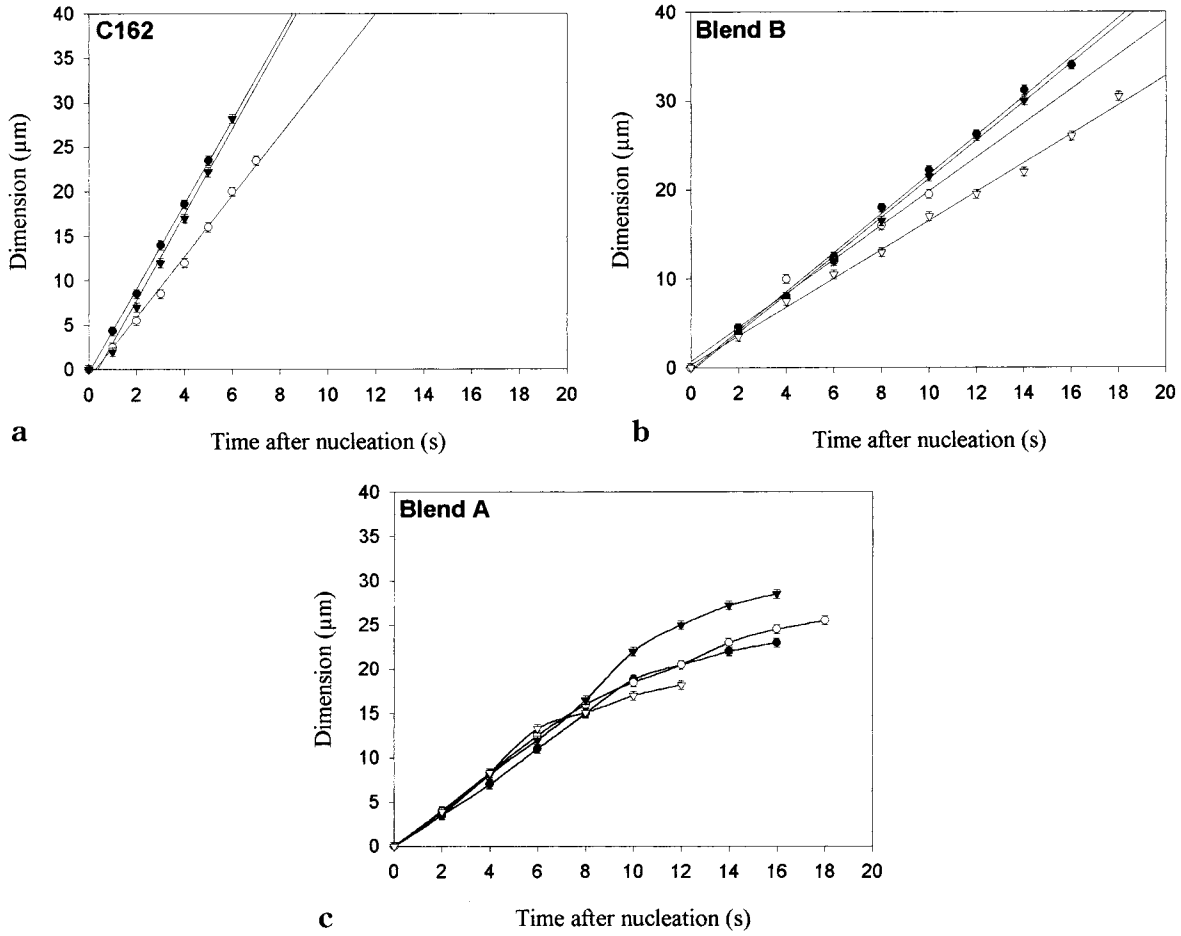

Figure 3. Crystal size as a function of crystallization time at 120 °C for (a) C162, (b) blend B, and (c) blend A.

is varied (cf. Figure 1, parts b and c), the shapes of the two exotherms are then very different. The crystallization time of blend B, (Figure 1c) is then noticeably greater than that of the blend A (Figure 1b) with crystallization ending rather abruptly for the former but gradually slowing for the latter. In addition, crystallization times are increased a little by going from 5% C246 to 10% C246 (Figure 1, parts c and d).

Growth Kinetics. When crystal growth rates are measured directly, the results are entirely consistent with the trends reported above. For those growth rates which do not change with time; a single average growth rate applies. Where the rate does change with time, for a simple first comparison, we shall use the initial growth rate in respect of those systems and discuss the time dependence in detail later.

Parts a−c of Figure 2 show, respectively, the crystal growth rate as a function of crystallization temperature for pure C162; the pair of 5% blends (A and B) and the pair of 10% blends (C and D). The apparent constant rate at lower temperatures in Figure 2a is an artifact, indicating that, in reality, crystallization is occurring above the indicated temperature. In blends A and C, whose growth rates were nonlinear with time, the data are of the initial growth rates; in all other systems the growth rate was linear. This plot confirms many of the trends identified by DSC previously; for example, in comparing either Figure 2b or Figure 2c with Figure 2a, the approximate halving of the growth rate is made clear. Moreover, the differences between the pairs of blends at the higher crystallization temperatures are very apparent. At 121 °C, the lowest isothermal crystallization temperature, the blend pairs have the same initial rate. Above this temperature, the growth rates of blends B or D decrease noticeably more than those of blends A and C. Increasing the amount of the second component (cf. Figure 2, parts b and c) reduces the growth rate such that the "cutoff", i.e., the extrapolated temperature for zero growth rate, is decreased; in the case of the pair of 10% blends (Figure 2c), the reduction is ∼1 K.

Use of the initial growth rates for blends A and C, although valuable for simple and meaningful comparisons between the blend pairs and showing that there is broad agreement with the DSC results, necessarily neglects the nonlinear behavior. This is shown in Figure 3, which contains several representative examples of both linear and nonlinear growth rates, at 120 °C, in which the raw data of crystal dimensions for individual objects are plotted against the time after nucleation. Figure 3a shows that the kinetics of C162 are constant with time, as is always true of all the pure paraffins. For C162, the single average growth rate is measured to be $4.2 \pm 0.5\ \mu m \cdot s^{-1}$. In both blends B and D, with the longer guest, the growth rate is also constant. Data for blend B, Figure 3b, give this as $2.1 \pm 0.5\ \mu m \cdot s^{-1}$. However, in the C122/C162 blends, nonlinear behavior occurs above the melting point of the guest, as shown, for example, in Figure 3c. Initial growth is at the same rate as that of blend B ($2.0 \pm 0.6\ \mu m \cdot s^{-1}$) but thereafter the growth rate halves to $1.1 \pm 0.3\ \mu m \cdot s^{-1}$. Nonlinear growth is only seen in blends A and C when they are crystallized above ∼119 °C i.e., roughly the melting point (119.5 °C) of the C122 minority component.[13]

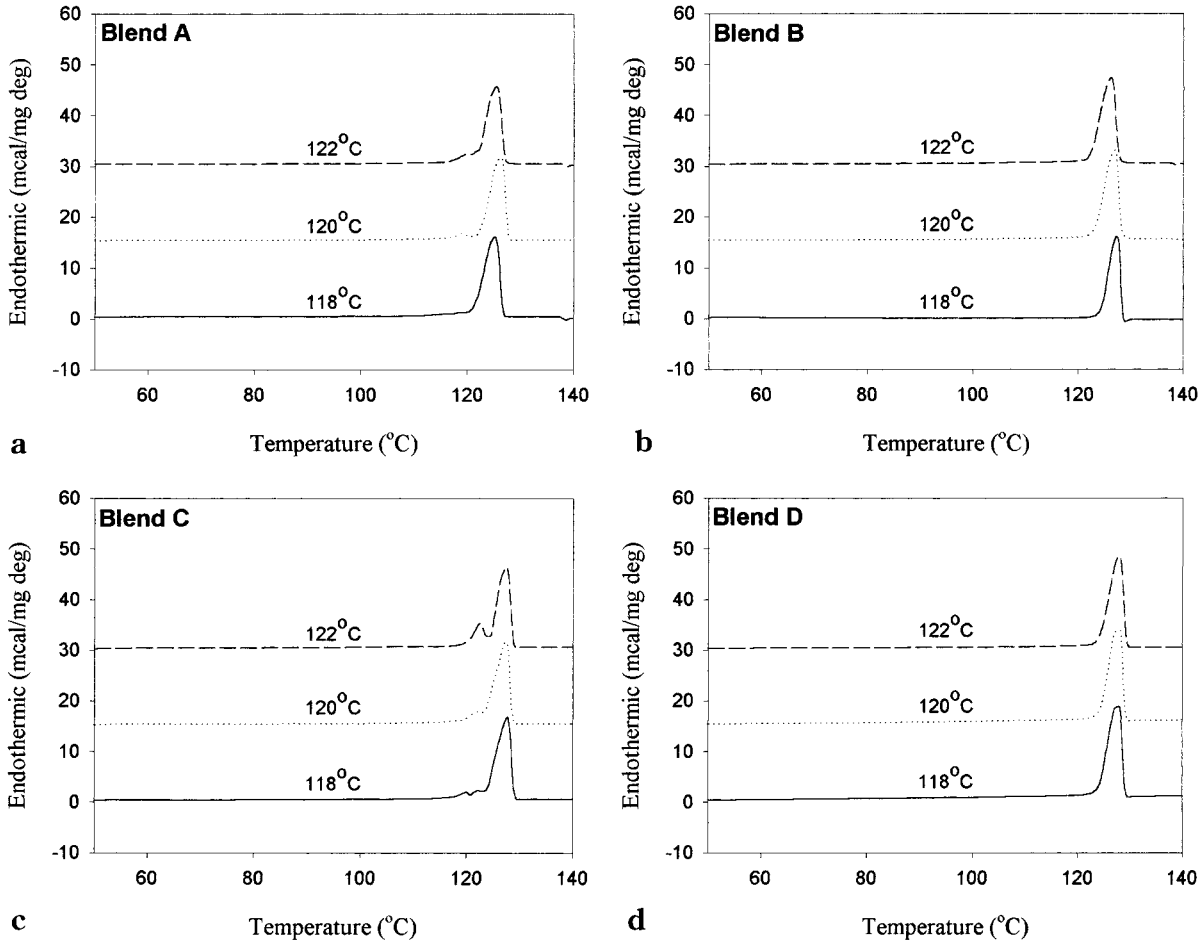

Figure 4. DSC melting endotherms for (a) blend A, (b) blend B, (c) blend C, (d) and blend D.

Accordingly, above this temperature, the C122 behaves as a noncrystallizable impurity, when it will accumulate at the interface with the melt[14] and contribute to the reduction in growth rate.

Melting Behavior. An illustrative set of DSC melting endotherms is shown in Figure 4 selected at three crystallization temperatures. Most traces show singular melting peaks at a temperature corresponding to a population of extended-chain crystals of C162. However, in blends A and C (Figure 4, parts a and c), two peaks are clearly present for crystallization above 119 °C, the lower corresponding to a separated population of C122 lamellae. This behavior and the associated nonlinear kinetics follow from the C122 in blends A and C being unable to crystallize at these temperatures, so that it is rejected from the growing crystals of C162 and, on cooling, forms a subsidiary population of C122 crystals. This lower peak, at the melting point of pure C122[13] is more apparent in blend C, which has the higher concentration of C122. The two lower peaks observed for blend C crystallized at 118 °C are somewhat different, and their precise nature has yet to be ascertained.

By contrast, in blends B and D (Figure 4, parts b and d), all the endothermic peaks are singular and the growth kinetics linear. This is strong evidence that the C246 has been incorporated into crystals of C162 to which it will add permanent cilia. There is no evidence for a separate population of C246 crystals in this blend whose detection would be well within the sensitivity of the DSC.

These results show clearly that the presence of a guest molecule causes the two blend pairs (A/C and B/D) to behave differently according to whether the guest is shorter or longer than the host. Thus, in blends A or C crystallized at 118 °C, little or no segregation occurs, growth rates are measured to be linear, and the crystal thickness is the same as that found in the pure paraffin, C162. Cocrystallization of the C122 and C162 appears to occur. By contrast when these same blends are crystallized above the melting temperature of C122, this alkane segregates resulting in nonlinear isothermal growth and a separate population of C122 crystals formed on cooling. There is no indication of segregation in blends B or D crystallized at all temperatures. For these the evidence clearly points to the crystals being of C162 ciliated by C246.

Results: Morphology

Optical Microscopy. Parts a–c of Figure 5 are micrographs of pure C162 crystallized at 118, 120, and 122 °C, respectively. The morphology is composed of *pseudo-spherulites*, that is, entities which, though more or less circular in section having been nucleated at a single center, lack the equivalent radii of classical spherulites, so that their textures when viewed through crossed polars differ markedly from the "Maltese cross" pattern. Instead, groups of lamellae in parallel array extinguish together between crossed polars but generally not along radii parallel to either of these directions because the *b* axis does not lie along them in that locality. With increasing crystallization temperature such objects become both larger, due to reduced nucleation, and coarser in texture. This is entirely consistent

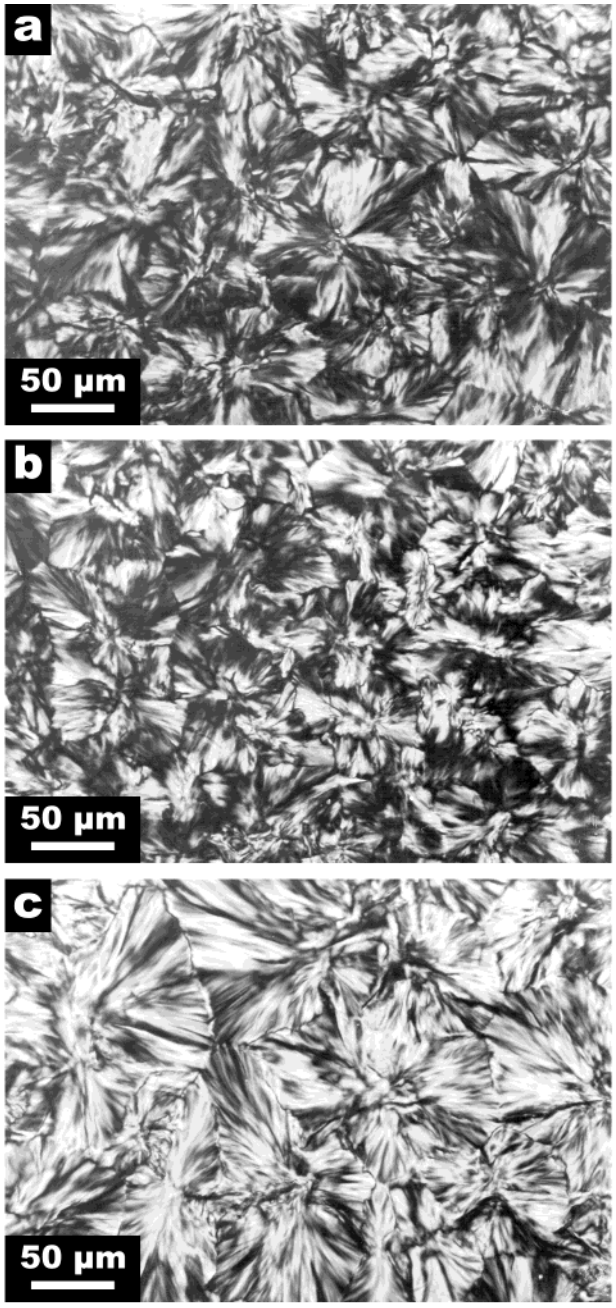

Figure 5. Optical micrographs, between crossed polars, of pure C162, crystallized at (a) 118, (b) 120, and (c) 122 °C. These are not truly spherulitic habits differing from them in the absence of the Maltese cross and the common extinction of wide areas.

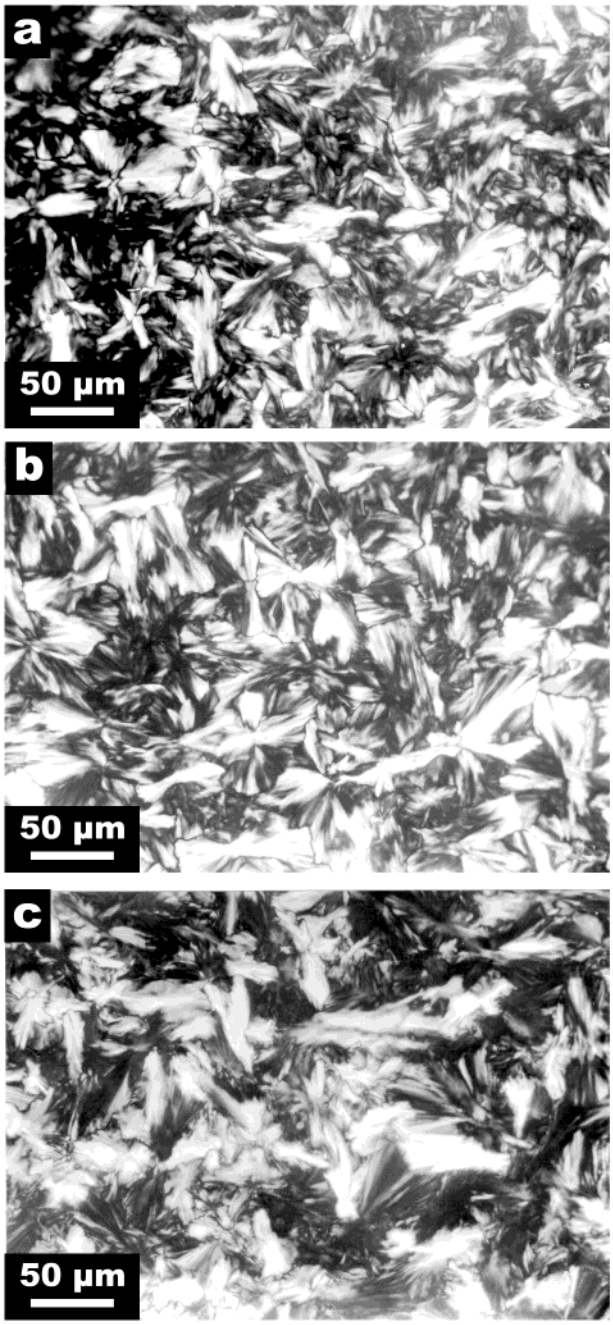

Figure 6. Optical micrographs, between crossed polars, of blend A, crystallized at (a) 118, (b) 120, and (c) 122 °C. In this blend the textural differences from classic spherulites noted above for the pure host are accentuated.

with the behavior of other extended-chain paraffins reported in detail elsewhere.[11−13]

Figure 6 shows equivalent micrographs from blend A. After crystallization at 118 °C (Figure 6a), the morphology is rather similar (but not identical and somewhat coarser in texture) to pure C162 crystallized at that temperature (Figure 5a). This is unsurprising, given the cocrystallization of both blend components at this temperature, allowing the minority, shorter component, C122, to be incorporated into a single crystal population. Above its melting point, however, the C122 becomes an uncrystallizable impurity which is rejected from the growing crystals, as is confirmed by DSC and growth rate data. This segregation changes the microstructure substantially for crystallization above 119 °C to one of coarse, randomly orientated crystal clusters; two examples are shown, in Figure 6, parts b and c, after crystallization at 120 and 122 °C, respectively. The coarser textures shown in Figure 6, parts b and c, in comparison to Figure 5, parts b and c, demonstrate unambiguously that, in this instance, the addition of an uncrystallizable component has disrupted, rather than facilitated, spherulitic growth.

Micrographs of blend B at the same three temperatures are shown in Figure 7. Systematic comparison with Figure 5 reveals that the morphology is composed of finely textured, spherical objects. Their extinction patterns are little affected when the sample is rotated between crossed polars, the implication being that the textural units are both finer in scale and more branched so that lamellae are able to grow more nearly radially.

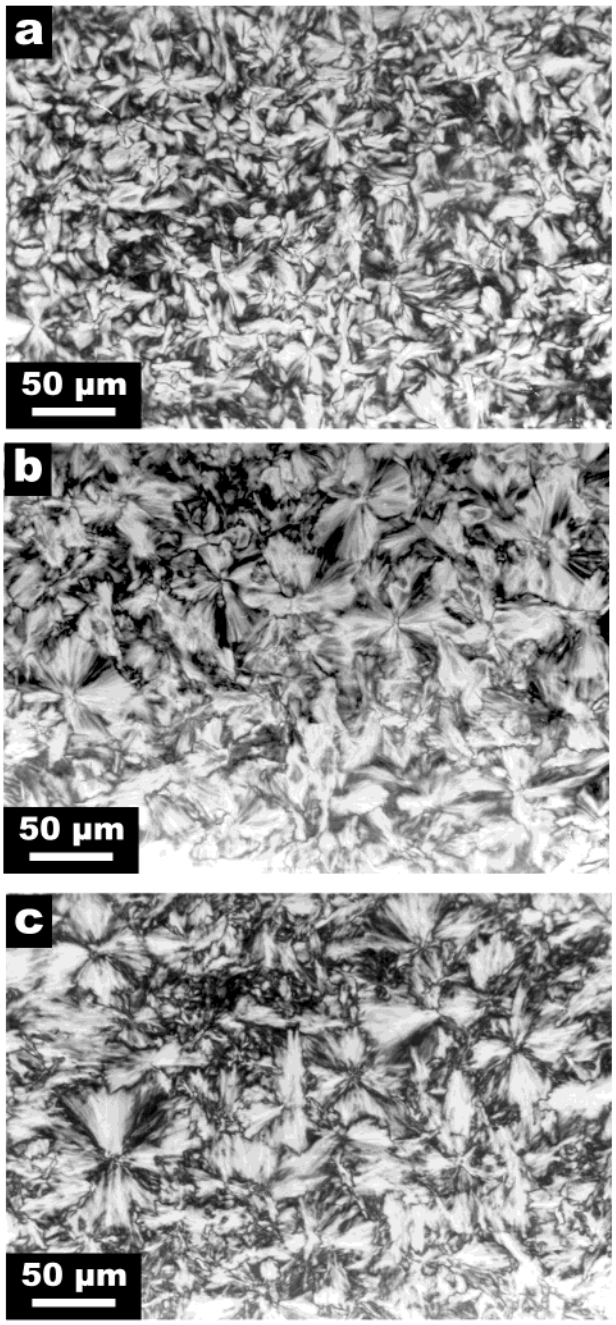

Figure 7. Optical micrographs between crossed polars of blend B crystallized at: (a) 118, (b) 120, and (c) 122 °C. With permanent ciliation textures are finer than for the host and tend to extinguish more nearly as radial units.

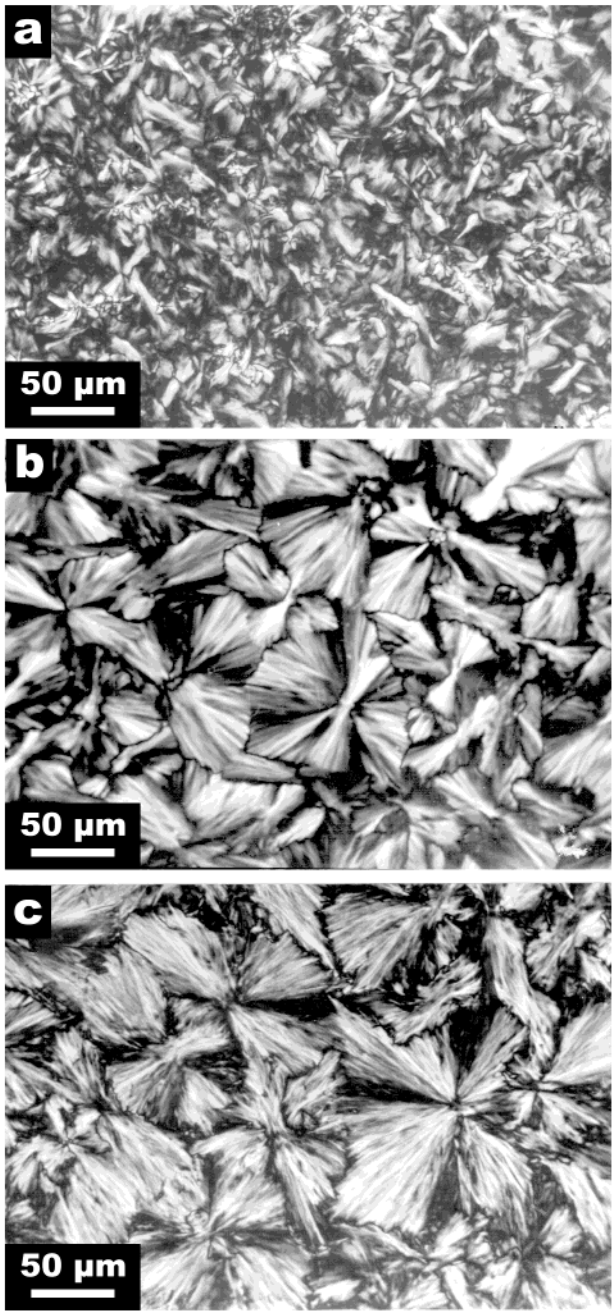

Figure 8. Optical micrographs, between crossed polars, of (a) blend C crystallized at 120 °C, (b) blend D crystallized at 120 °C, and (c) blend D crystallized at 122 °C. The texture of the first of these, with the shorter guest molecules, is still far from truly spherulitic while the last two, with permanent ciliation, do approach the appearance of classic spherulites, with Maltese cross, quite closely.

By contrast a sample of pure C162, similarly rotated, shows abrupt changes of contrast as packets of lamellae extinguish as a whole. These blend objects also become larger, with a coarser texture, at higher temperatures of crystallization (Figure 7c) because of reduced primary nucleation.

Figure 8 shows three representative examples of the 10% blends which have very similar textures to the two 5% blends considered previously. For example, segregation of C122 above its melting point produces a nearly identical disruption of lamellar microstructure in blend C (Figure 8a) to that found for blend A (Figure 6b). In blend D, the increased C246 content and associated greater degree of ciliation give a still finer texture to spherulites with the extinction pattern between crossed polars yet more akin to the classic "Maltese cross" (Figure 8, parts b and c). These results, for which cocrystallization of a small percentage of a longer molecule generates permanent cilia, demonstrate very clearly that the presence of such cilia promotes a spherulitic texture.

TEM Study. Although the predominant evidence cited in this paper is of larger scale morphologies, a limited number of representative micrographs are shown to provide the underlying lamellar detail and, in particular, the interlamellar organization. When a C122/C162 blend is crystallized with segregation of the C122 the result is a texture composed of lamellar stacks (Figure 9a) with little internal lamellar divergence

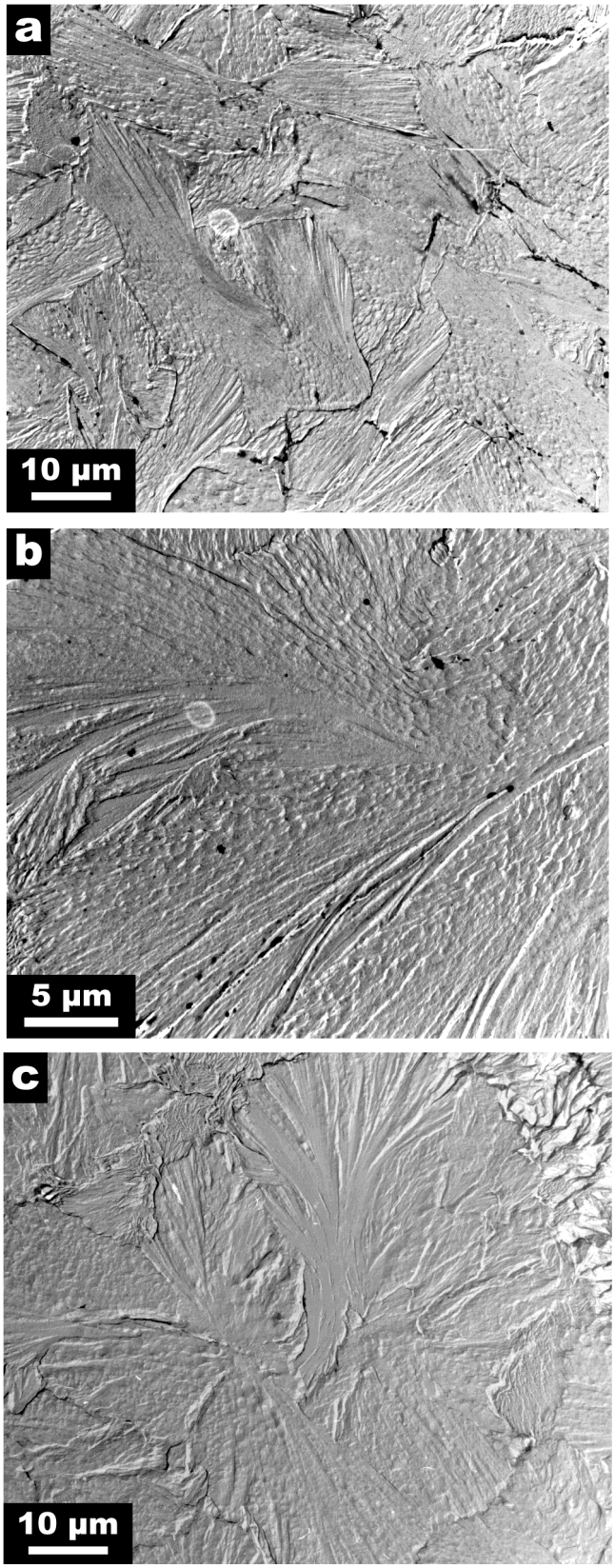

Figure 9. TEM micrographs of (a) blend A crystallized at 120 °C, (b) blend A crystallized at 118 °C, and (c) blend B crystallized at 118 °C. The lamellar arrangements underlying the previous optical textures have small divergence for blend A, though increasing with supercooling (lower temperature) while blend B shows a greater divergence of finer units.

apparent, any present being confined to low angles <5°. There is more divergence when C122 is not segregated, i.e., for crystallization at 118 °C and below, (Figure 9b), more akin to that reported for the pure paraffins.[13] This morphology is distinct from that of the C246/C162 blends crystallized at the same temperature where distinctly spherulitic structures are obtained, constructed on a dominant/subsidiary basis with divergence angles of ~20° between adjacent crystals as in Figure 9c.

Some quantification of the variation of divergence angle between adjacent dominant lamellae as a function of supercooling is presented in Figure 10. Figure 10a refers to the 5% blends; Figure 10b, to the 10% ones. Both show the same character. In all cases the plots have a finite intercept, which is less for the shorter guest molecule (blends A, C) than for the longer one (blends B, D). Moreover the slope is less for all blends than for pure C162 and decreases as the proportion of guest molecules increases. Splaying is greater or less than for the pure host for blends with the longer and shorter guest molecules, respectively. These features are in accord with the expectation for ciliation as discussed below.

Discussion

The comparison of dilute blends of guest molecules in C162 with the pure *n*-alkane allows the kinetic and morphological consequences of ciliation and segregation to be studied with more control than was formerly possible. Following studies of polymer morphology, ciliation was assumed to occur during attachment of a long molecule to a growing crystal and to provide a transient repulsive force on an adjacent lamella causing it to diverge from its parent and then, for separations greater than cilium lengths, to grow without further applied stress.[15] In the *n*-alkane examples studied there is strong supporting circumstantial evidence for this scenario. Not only was the anticipated major difference in lamellar packing observed between chainfolded and extended-chain growth related to the presence and absence of cilia, but also the increasing divergence of extended-chain lamellae at higher supercoolings was measured to be linearly dependent on this variable, i.e., proportional to the extended length of a cilium. However, the much shorter lengths of alkane cilia and the observed finite splaying at zero supercooling suggest that surface roughness of the embryonic lamella also contributes to splaying. The experiments of this paper, in which permanent cilia have been produced by blending two monodisperse systems, have produced complementary evidence which strongly reinforces the case for the involvement of ciliation (and possibly also of surface roughness) in causing lamellar splaying and thence spherulitic growth in polymers and confirm the independence of this characteristic phenomenon from cellulation.

The kinetic data emphasize the importance of the conformations of molecules attached to the growth face. Equal reductions in growth rate for cocrystallization of both longer and shorter guest molecules—for which the small changes in supercooling would be of opposite sign—indicate that the net rate of attachment of molecules to a lamella has lessened. Likely mechanisms are, for a shorter guest, first, a greater extent of detachment of stems back into the melt[16] and, second, interference with the host molecules by provision of partial stem vacancies which the host may penetrate and so delay its attainment of the correct conformation. For a longer guest, probably one need look no further than interfer-

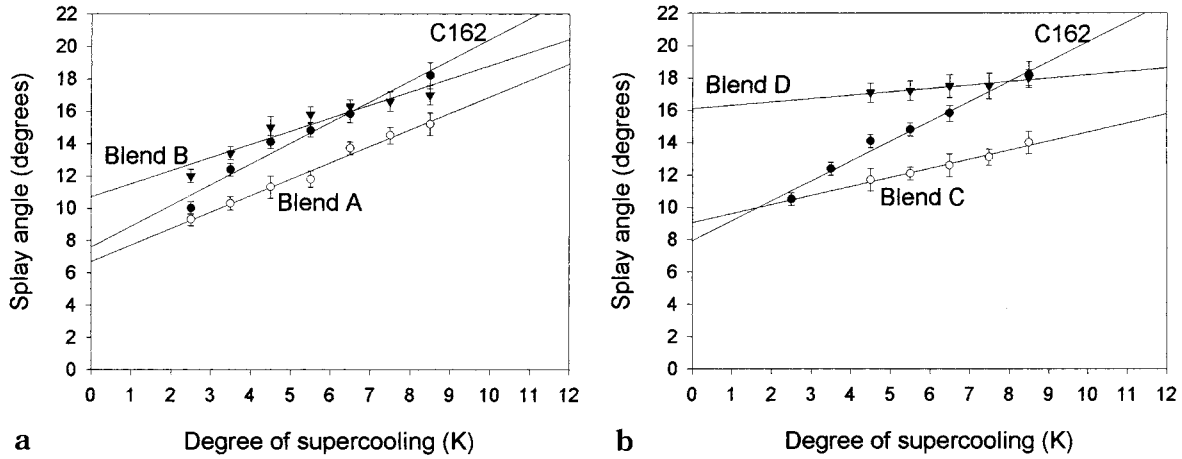

Figure 10. Angles between adjacent dominant lamellae plotted as functions of supercooling for pure C162 with (a) the 5% blends (A and B) and (b) the 10% blends (C and D).

ence of the associated cilia with the addition of host molecules for the rate reduction. This suggestion and that below concerning segregated molecules, now extend the hypothesis of so-called "self-poisoning" proposed[17] initially to explain the growth rate minimum associated with a change from one quantized conformational state of the *n*-alkanes to another, to kinetics within one such state.

A constant isothermal growth rate, found both for the pure host and the cocrystallizing blends, is indicative of steady-state conditions pertaining at the interface. The nonlinear growth, on the other hand, is evidence of segregation and, as in other cases studied recently,[14,18] shows a monotonic decrease until a steady state is established, with constant segregant concentration at the interface.

The optical morphologies are complex but clearly move toward the classic spherulitic condition of equivalent radii with an associated "Maltese cross" with increasing addition of the longer guest. The shorter guest, on the other hand, even in conditions above its melting point when it segregates as a noncrystallizable "impurity" does not effect a comparable change. A comparison of Figures 5c and 6c would suggest that rather than promoting spherulitic growth, as was once suggested,[19] segregation disfavors it, at least in these systems.

At this point it is pertinent to note that there is no language which adequately describes the manifold complexities of the spherulitic state and especially not the gradual and subtle changes, involving both increased splaying and more frequent branching, from effectively single-crystal blocks toward the classic morphology of crystallographically equivalent radial units such as we have encountered in this paper. What is required is parametrization of the morphology toward which goal, the data of crystal splaying shown in Figure 10 represent a first step. The behavioral trends displayed accord with straightforward expectation of both permanent and transient ciliation coupled with some additional features related to lamellar surface condition and "poisoning" of the growth face by segregated molecules.

The proposal to date is that in crystallization of a pure alkane there will be a stage in which a proportion of chain, the length of the secondary nucleus will be attached to the crystal leaving the remainder as a transient cilium. The splaying data for C162 and that for C122 and C246 published previously[13] are linear with supercooling and, on the above basis, extended cilium length. The actual lengths are small, a few nanometers at most, indicating that their effect must be confined to the region very near a branch point. This inference is more precise than was possible for polymers with their much longer molecular lengths. Such small dimensions imply that not only will molecules adding to side surface be able to affect the packing of adjacent basal surfaces but there also will be an additional factor. This is that at the inception of a new layer its surface packing will be rougher than that which develops over time because of the relatively small decrease in free energy which improved surface packing is able to contribute. An embryonic layer with a rough basal surface will not be able to pack well with its neighbor and so tend to repel itself therefrom producing mutual divergence.[20] The positive intercept in Figure 10 is support for this mechanism which would contribute to finite divergence at zero supercooling and cilium length. Both ciliation and surface roughness would thus participate in causing adjacent lamellae to diverge.

In considering the implications of the data shown in Figure 10 we note, first, the behavior of the pure host shows splaying proportional to cilium length and a positive intercept suggestive of the influence of surface roughness as discussed above. The contribution to splaying of permanent cilia of fixed length will be independent of supercooling so that the combination of transient and permanent ciliation would be expected to give greater splaying angles but with a lesser slope than the purely transient ciliation of the host. Not only is this the case for blends B and D in Figure 10, parts a and b but also the further reduction in slope for the blend D is as expected for a greater number of permanent cilia.

If one attempts to separate the relative effects of transient and permanent cilia, it is immediately clear that they do not add in simple proportion to the blend composition, nor would this be expected to be the case. This follows because the 82 C atom excess length of the C246 guest over the C162 host would, if present in nonoverlapping random-coil conformations, be more or less sufficient to cover the basal surface at 5% concentration. Even such a small proportion of cilia would thus be expected to have a major effect on the basal surface environment.

When the guest molecule is shorter than the host, Figure 10 shows that splaying is depressed compared with the host especially at the higher supercoolings at which it is segregated, and more so for blend C with the higher guest concentration. This reduction, which will lessen the tendency to spherulitic growth, may tentatively be ascribed to the reduction in transient ciliation brought about by "poisoning" of the growth surface by the segregated species in a way which needs elucidation.

Conclusions

The four principal conclusions of this paper are as follows:

1. Blends with a guest either longer or shorter than the host molecule reduce the crystallization rate because of competing processes at the crystal/melt interface.

2. Cocrystallization with a longer guest molecule, producing permanent cilia, increases splaying angles and enhances spherulitic growth, giving a finer-textured product tending toward the classic condition of crystallographically equivalent radii.

3. Segregation of a shorter guest molecule reduces splaying angles and disfavors spherulitic crystallization.

4. In all cases, adjacent dominant lamellae splay apart by angles which increase linearly with supercooling with a positive intercept at zero supercooling. The rate of increase is less for blends than for the pure host and the magnitudes increase with guest concentration. The greatest effect occurs when there is permanent ciliation; the least, when the guest molecule segregates. The latter is tentatively ascribed to reduced ciliation due to poisoning of the growth interface by the segregated molecules.

Acknowledgment. This research was funded by EPSRC under whose auspices the *n*-alkanes were synthesized and supplied by Dr. G. M. Brooke and colleagues at the University of Durham.

References and Notes

(1) Keller, A In *Growth and Perfection of Crystals*; Doremus, R. H., Roberts, B. W., Turnbull, D., Eds.; Wiley-Interscience: New York, 1958, p499.
(2) Bunn, C. W.; Alcock, T. C. *Trans. Faraday Soc.* **1945**, *41*, 317.
(3) Bassett, D. C.; Keller, A.; Mitsuhashi, S. *J. Polym. Sci. Part A* **1963**, *1*, 763.
(4) Bassett, D. C.; Olley, R. H. *Polymer* **1984**, *25*, 935.
(5) Bassett, D. C.; Vaughan, A. S. *Polymer* **1985**, *26*, 717.
(6) Bassett, D. C.; Olley, R. H.; al Raheil, I. A. M. *Polymer* **1988**, *29*, 1539.
(7) Paynter, O. I.; Simmonds, D. J.; Whiting, M. C. *J. Chem. Soc., Chem. Commun.* **1982**, 1175.
(8) Bidd, I.; Holdup, D. W.; Whiting, M. C. *J. Chem. Soc., Perkin Trans* **1987**, *1*, 2455.
(9) Ungar, G.; Stejny, J.; Keller, A.; Bidd, I.; Whiting, M. C. *Science* **1985**, *229*, 386.
(10) Bassett, D. C.; Olley, R. H.; Sutton, S. J.; Vaughan, A. S. *Macromolecules* **1996**, *29*, 1852.
(11) Bassett, D. C.; Olley, R. H.; Sutton, S. J.; Vaughan, A. S. *Polymer* **1996**, *37*, 4993.
(12) Teckoe, J.; Bassett, D. C. *Polymer* **2000**, *41*, 1953.
(13) Hosier, I. L.; Bassett, D. C. *Polymer* **2000**, *41*, 8801.
(14) Abo el Maaty, M. I. *Polym. J.* **1999**, *21*, 778.
(15) Bassett, D. C. *Philos. Trans. R. Soc. London Ser. A.* **1994**, *348*, 29.
(16) Hoffman, J. D.; Miller, R. L. *Polymer* **1997**, *38*, 3151.
(17) Ungar, G.; Keller, A. *Polymer* **1987**, *28*, 1899.
(18) Abo el Maaty, M. I.; Bassett, D. C.; Olley, R. H.; Jääskeläinen, P. *Macromolcules* **1998**, *31*, 7800.
(19) Keith, H. D.; Padden, F. J. *J. Appl. Phys.* **1963**, *34*, 2409.
(20) Bassett, D. C. *Polym. J.* **1999**, *31*, 759.

MA000946T